

# An Advanced Methodology to Enhance Energy Efficiency in a Hospital Cooling-Water System

Eduardo Dulce-Chamorro<sup>1,\*</sup>, Francisco Javier Martinez-de-Pison<sup>a</sup>

<sup>a</sup>EDMANS Group, Department of Mechanical Engineering, University of La Rioja, Logroño, Spain.

---

## Abstract

Healthcare facilities consume massive amounts of energy. This study outlines a methodology to enhance energy efficiency and solve common problems in hospital cooling-water systems, since hospitals are the most energy-intensive type of building. Building Management Systems (BMS) are a widely used technique to control and monitor all the different energy facilities contained in hospitals. Proper setup and upgrades can resolve inefficiencies and existing problems. The methodology described herein addresses the general cooling system adjustments in three main areas: control system (CS), data acquisition system (DAS), and physical system (PS). An innovative feature incorporated in this methodology is the cooling demand model integrated into the CS, which is capable of forecasting and transmitting a schedule for maximum thermal energy requirements to the BMS a day in advance, thereby anticipating decisions and scheduling energy generation and maintenance operations. During the process of developing the cooling demand model, various machine learning models were trained. This process consisted of searching for low-complexity models using a methodology called *GAparsimony*. This methodology uses genetic algorithms to search for highly precise, robust models that use a low input. The final model consisted of a weighted combination of Artificial Neural Network (ANN) and Support Vector Regression (SVR) models. The energy savings obtained thanks to this methodology are estimated to be between 7% and 10% per year. The energy plant improved its performance and chiller starts were reduced by 82.5%. It should also be noted that this study was affected by the recommendations for increased ventilation due to the COVID-19 pandemic, which entailed a 22.4% increase in energy consumption in 2020. The methodology was developed and tested successfully in a real hospital BMS between 2017 and 2019; the model was finally integrated in 2020.

**Keywords:** Cooling demand forecasting, Building Management Systems (BMS), Energy efficiency, *GAparsimony*, Parsimonious modeling, Ensemble algorithms.

---

## 1. Introduction

2 The Paris climate accord (signed April 22th, 2016) was designed to keep global tem-  
3 perature rise below 2 °C above pre-industrial levels and to limit that increase even further  
4 to 1.5 °C [1]. This goal requires that global carbon emissions drop as soon as possible, in  
5 order to "achieve a balance between anthropogenic emissions by sources and removals by  
6 sinks of greenhouse gases". In accordance with this agreement, on November 28th, 2018 the  
7 European Commission published its Climate Strategies [2]: establishing greenhouse-gas-  
8 emissions reduction targets for 2020, key laws and measures to achieve their goals for 2030,

---

\*Corresponding author

Email address: edulce@riojasalud.es (Eduardo Dulce-Chamorro)

9 and the long-term objective of a climate-neutral European Union (EU) by 2050. That is,  
10 by 2050, the EU will reduce its emissions by 80%, to below 1990 levels. More recently, the  
11 UN Climate Change Conference COP25 (2~13 December, 2019) took place in Madrid with  
12 the purpose of following up on the implementation of the Paris agreement guidelines and  
13 build prospects ahead of 2020.

14 European buildings are the greatest consumers of energy and are responsible for ap-  
15 proximately 40% of the EU's total energy consumption of its CO<sub>2</sub> emissions [3] and 36%.  
16 Improving the efficiency of existing buildings could potentially lead to significant energy  
17 savings and lower CO<sub>2</sub> emissions by about 5%, in the case of both total energy and CO<sub>2</sub>  
18 emissions.

19 The International Energy Agency (IEA) has found that cooling is the fastest-growing  
20 end-use of energy in buildings, as the energy demand of cooling systems more than tripled  
21 between 1990 and 2018, reaching around 2,000 TWh of electricity [4]. The increase in cool-  
22 ing demand is impacting power generation and distribution capacity, especially during  
23 peak-demand periods and extreme-heat events. Space cooling in buildings is responsi-  
24 ble for 50% of peak electricity demand. CO<sub>2</sub> emissions from space cooling are also rising  
25 rapidly, tripling between 1990 and 2018 to reach 1,130 million tons. Air conditioning ac-  
26 counts for nearly 20% of total electricity use in buildings around the world today [5].

27 This study focuses on a chilled-water installation because of its essential role in hos-  
28 pitals for healthcare activities: Air Conditioning (AC) in operating rooms, intensive care  
29 units (ICU), emergency rooms, etc. It is also fundamental for operating medical equipment  
30 such as that used in radiology and diagnostic imaging, scanners, refrigeration storage in  
31 blood bank, kitchens, and pharmacies; pathology, the morgue, and laboratories. Computer  
32 and data center racks also require cooled water. Studies have shown that the energy re-  
33 quired by chilled-water installations and AC in a medical building constitutes 40% to 45%  
34 of the total energy necessary [6, 7]. Hospitals can decrease their energy consumption by  
35 more than 20% by implementing a BMS, adequately zoning for AC, adding measurement  
36 sensors in different areas, analyzing historical data from those systems, planning proper  
37 use schedules, harnessing energy from extraction air and regulating the speed of fans and  
38 water pumps.

39 The methodology presented herein enhances energy efficiency and solves common prob-  
40 lems in hospital cooling plants. Its foremost innovation is that it incorporates a predictive  
41 model of thermal cooling demand to the BMS that can forecast the activity of the water-  
42 cooled generators. The model integrated into the BMS creates a predicted schedule for the  
43 day ahead for the cooling generators. The optimized system is capable of reducing ineffec-  
44 tive starts and stops that can otherwise lead to costly breakdowns and inefficient electrical  
45 starting peaks.

46 This study has shown that the methodology proposed is effective in improving the  
47 building's energy efficiency, optimizing the electrical consumption of cooling systems, de-  
48 creasing CO<sub>2</sub> emissions, contributing to the thermal comfort of users, and minimizing  
49 maintenance costs through the use of machine learning techniques.

### 50 1.1. Related studies

51 In the past some interesting related studies have been conducted to predict thermal  
52 demand in buildings using different forecasting techniques: linear regression for estimat-  
53 ing cooling energy of condominiums [8], combining ANN with an ensemble approach or  
54 clustering-enhanced adaptive ANN to forecast building cooling loads [9, 10], Artificial

55 Intelligence (AI) to predict energy consumption of Low Energy Buildings (LEB) [11], and  
56 hybrid approach for building stock energy prediction [12].

57 Likewise, electrical demand models have been designed to predict the energy consump-  
58 tion of Heating, Ventilation and Air Conditioning (HVAC) systems applying different tech-  
59 niques: algebraic modeling [13], ANN [14], an ANN comparison with Random Forest (RF)  
60 [15], and SVR [16]. In a field related to the present study, research has been conducted to  
61 forecast electrical consumption in hospital facilities based on ANN [17].

62 Model Predictive Control (MPC) applications for HVAC models have been tested with  
63 ANN models [18, 19], including a MPC formulation framework for Enhancing Building  
64 and HVAC System Energy Efficiency [20].

65 Some recently published methods have automated and facilitated modeling processes  
66 with hyperparameter optimization (HO) and feature selection (FS) in [21, 22]. The GAparsimony  
67 methodology used in this study is a genetic algorithm (GA) that conducts parsimonious  
68 model selection (PMS) [23]. It has been successfully applied in a range of contexts such as  
69 steel industrial processes [24], hotel room booking forecasting [25], mechanical design [26],  
70 and solar radiation forecasting [27].

71 This article presents a new methodology that has been successfully applied in an ac-  
72 tual large-sized hospital to improve energy efficiency and performance by forecasting the  
73 thermal energy demand of the cooling-water system. The final model integrated into the  
74 BMS is an ensemble model comprised of the best SVR and ANN models built with the  
75 GAparsimony methodology for parsimonious modeling. The optimizations and the appli-  
76 cation of the improvements were carried out over the past three years. The results were  
77 integrated, tested and measured during 2020.

## 78 2. Case study description

### 79 2.1. Main hospital description

80 The San Pedro Hospital is the foremost hospital in the region of La Rioja (Spain) and  
81 belongs to the Spanish national public healthcare system. The area of the hospital is about  
82 126,057.83  $m^2$  and has seven above-ground floors.

83 As the primary hospital in the area, it offers a wide range of medical services, the most  
84 energy-demanding of which are: over 600 beds for hospitalization (which were fully occu-  
85 pied during the first wave of COVID-19), a diagnostic imaging area, 23 operating rooms, an  
86 emergency area with 40 beds, hemodialysis, two ICUs with 32 beds (one of them adapted  
87 during the COVID-19 crisis), endoscopy, laboratories, pharmacy, sterilization, and other  
88 general services.

### 89 2.2. Technical description of the cooling system

90 Hospital's high voltage facilities, water tanks, emergency generators, storage of medical  
91 gases, cold-water production system and heating installations are centralized in a separate  
92 building and then distributed by a ring pipe around the basement of the building.

93 The cooling generation system under study consists of three centrifugal chiller units of  
94 3.51 MW, namely the *Trane CVFG* model (herein designated as EF1, EF2, EF3), and another  
95 screw machine of 1 MW cooling capacity, namely the *Trane RTHD* model (designated as  
96 EF4). Figure 1 shows the hydraulic schema of the water-cooling facility.

97 The BMS is comprised primarily by controllers belonging to the *Sauter EY3600* family.  
98 The BMS interface is a SCADA application with a *novaPro Open 4.1.* environment. The

99 existing BMS controlled the system on a real-time basis, using information captured by  
100 sensors and ordering actions to the actuators when temperature set-points exceeded pre-  
101 determined values.

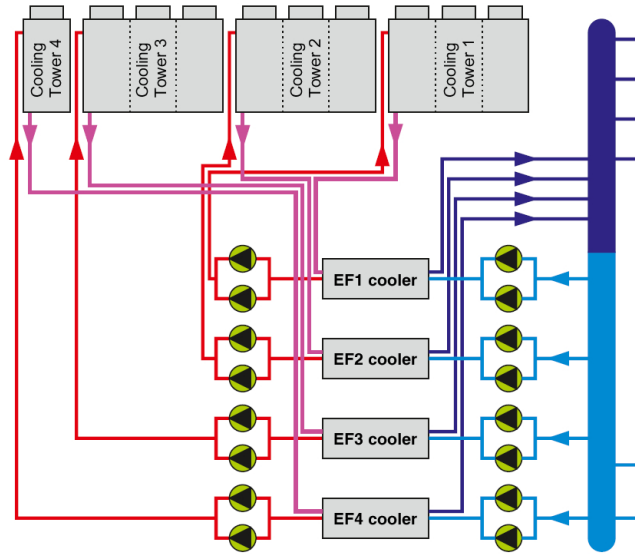


Figure 1: Hydraulic schema of cooling-water-generation system.

### 102 2.3. Past problems in the cooling system

103 Before starting the optimization process, the following malfunctions were detected:

- 104 - Inefficient and repeated starts and stops of the cooling generators, which were controlled exclusively by the water-distribution temperature set-point. This malfunction impacted energy efficiency negatively and can lead to significant breakdowns. The top manufacturers recommend that the maximum number of starts in scroll type compressors be under 12 per hour, and 6 in compressors equipped with inverters [28]. In addition, it is recommended that the working time after a chiller starts be at least 60 minutes.
- 105
- 106
- 107
- 108
- 109
- 110
- 111 - Inefficient maintenance expenses incurred because of a lack of a daily schedule. The system required having all the cold-water pumps ready for a start signal from the chillers. This fact entailed high maintenance costs because operating all the cooling towers required expensive antimicrobial and chemical treatments.
- 112
- 113
- 114
- 115 - Subcooling-water-ring temperature below established set-points diminished energy efficiency, e.g. two chillers begin operating simultaneously when only one of them was necessary.
- 116
- 117
- 118 - Overheating-water-ring temperature above established set-points owing to sudden chiller stops, which adversely affected healthcare services.
- 119



### 120 3. Methodology

121 The methodology provides a structured process to review all the main aspects related  
122 to the cooling-water system. As a final step, a forecasting demand model was implemented  
123 that can transmit the maximum energy required for the next day to the BMS. The process,  
124 which started in 2017, began with a deep optimization of the installation, the goal being to  
125 solve the problems described in Subsection 2.3. A timeline of the study and the stages of  
126 the methodology is depicted in Figure 2.

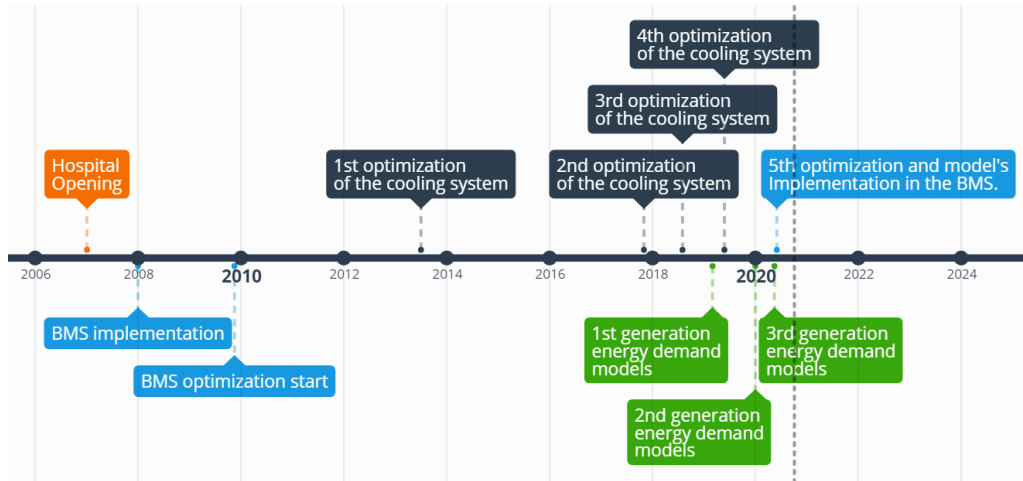


Figure 2: Case study timeline indicating the most influential improvements, model generations and implementation of the model inside the BMS.

#### 127 3.1. Control system improvements

128 These enhancements are applied to the control system and affect the set-points, the  
129 behavior of the field elements and actuators, the operating schedules and the predictive  
130 control systems that could be integrated.

131 The main facilities of the hospital are controlled by the BMS system. It was implanted  
132 in 2008, one year after the hospital opening. Since 2010 on-going optimization of the BMS  
133 has been underway in three main areas: lighting (adding sensors and schedules), HVAC  
134 distribution adjustments (adding sensors, and implementing schedules in fan coils, air con-  
135 ditioners, and pumps), heating generation (implementing schedules in pumps, optimizing  
136 the system).

137 The 1<sup>st</sup> optimization of the cooling system was developed before this study. It imple-  
138 mented a stepped set-point temperature of the cold-water ring (TCONSIG) that was calcu-  
139 lated depending on the outside temperature, instead of a fixed value, as beforehand.

140 In the 2<sup>nd</sup> optimization, a minimum working time for the water-cooled generators was  
141 established of at least one hour, and a cyclic order of use for the chillers was set up. This  
142 optimization significantly improved the behavior of the cooling-water generation system  
143 as can be observed in Figure 10 (from April 2018): the number of starts and stops in the  
144 chillers decreased dramatically. The improvement can also be appreciated in Figure 17,  
145 which depicts the number of starts of chillers.

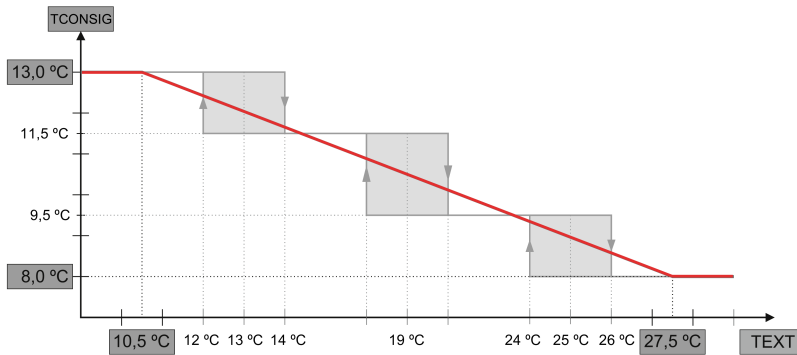


Figure 3: Set-point temperature of the cooling generation system (TCONSIG) calculated with the Exterior Temperature (TEXT) and modified in the third optimization from a stepped set-point to a linear one.

146 In the 3<sup>rd</sup> optimization, a linear set-point temperature of the cold-water ring (TCONSIG)  
 147 was applied and, in this optimization, calculated in proportion to the outside temperature  
 148 (TEXT) instead of as a stepped variable, as can be seen in Figure 3.

149 A supervised control system was implemented in the 5<sup>th</sup> optimization, described in  
 150 Subsection 3.4. The model communicates the maximum cooling-power demand for the  
 151 next day to the BMS and allows the system to foresee how many chillers will be necessary.  
 152 This also provides a schedule that allows planning for which chillers will be in operation,  
 153 optimizing energy efficiency and planning maintenance operations. In Figure 4, the contri-  
 154 bution of EF4 (1 MW) chiller to EF3 (3.5 MW) can be appreciated: these two chillers work  
 155 in conjunction to best fit the power generation to the day's maximum demand, instead of  
 156 starting two of the 3.5 MW chillers and subcooling the ring temperature.

157 Additionally, in this final step, a new generation schedule was implemented for Sum-  
 158 mer and Winter to adjust the demand to the appropriate chiller capacity. The scheduling  
 159 establishes separate day and night programs in Summer. Night programming establishes  
 160 the priority of use of the small chiller EF4 if the outside temperature is below 17 °C. The  
 161 winter schedule is similar to the summer-night program.

### 162 3.2. Improvements in the data acquisition system

163 These improvements affect the information acquisition and data processing system, as  
 164 well as the measurement systems.

165 Local Operating Network (LON) communication cards were installed in every genera-  
 166 tor in the 4<sup>th</sup> optimization to improve the internal adjustments of the chillers that the BMS  
 167 had not been able modify before. These communication cards allow the BMS to monitor  
 168 the internal operating parameters of the machine and modify the working conditions and  
 169 limits. They allow the set-point to be modified and limit the electrical power of each gen-  
 170 erator. This enables the machine's consumption to be adjusted according to the immediate  
 171 needs of the facility. The maximum power limitations of EF1, EF2, and EF3 were upgraded  
 172 from 70% to 90%, thereby providing a maximum cooling power greater than 3 MW per  
 173 chiller.

174 Furthermore, after these cards were set up, the quality and quantity of data recorded  
 175 improved dramatically in terms of precision as compared to data recorded with external  
 176 sensors, as can be observed in Figures 4 and 5.

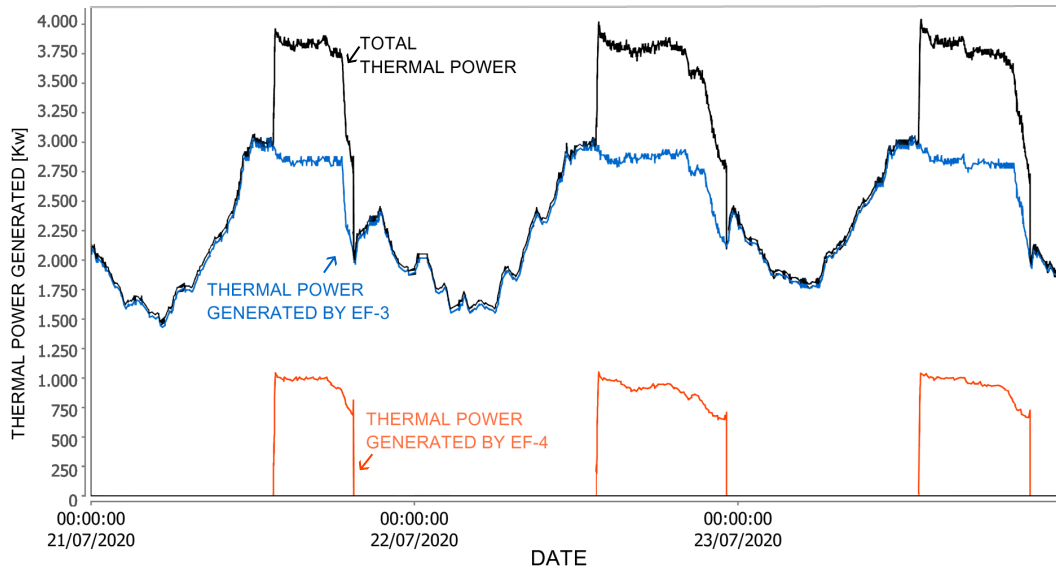


Figure 4: Cooling power generated July 21st – 23th , 2020. The reinforcement obtained by EF3 plus EF4 chiller to fit the demand can be observed. Data extracted from LON Cards installed in the 4<sup>th</sup> optimization.

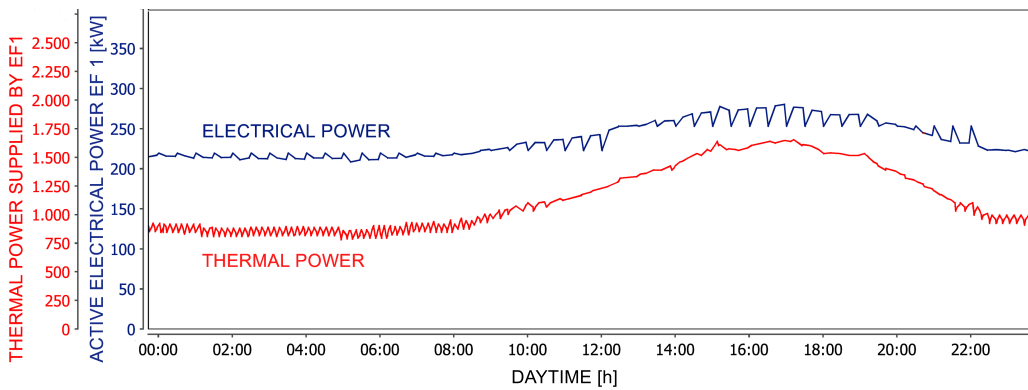


Figure 5: Thermal power generation of EF1 chiller data obtained with LON cards installed in the 5<sup>th</sup> optimization.

177 In the 5<sup>th</sup> optimization, electrical power meters were installed and integrated into the  
178 BMS system to measure the instantaneous consumption of each chiller. The impact of in-  
179 tegrating these power meters can be visualized in Figure 5. This improvement made it  
180 possible to analyze the efficiency of each machine while in operation.

### 181 3.3. Improvements in the physical system

182 These improvements are made by integrating new physical systems into the existing  
183 installation.

184 A frequency inverter system was installed in the EF4 screw type generator in the 4<sup>th</sup>  
185 optimization. The frequency inverter (AFD) can regulate the speed of the compressor with  
186 a partial load. In the EF1, EF2, and EF3, which are centrifugal chillers, AFDs could not be  
187 installed, nevertheless they still have a modulation with the refrigerant charge.

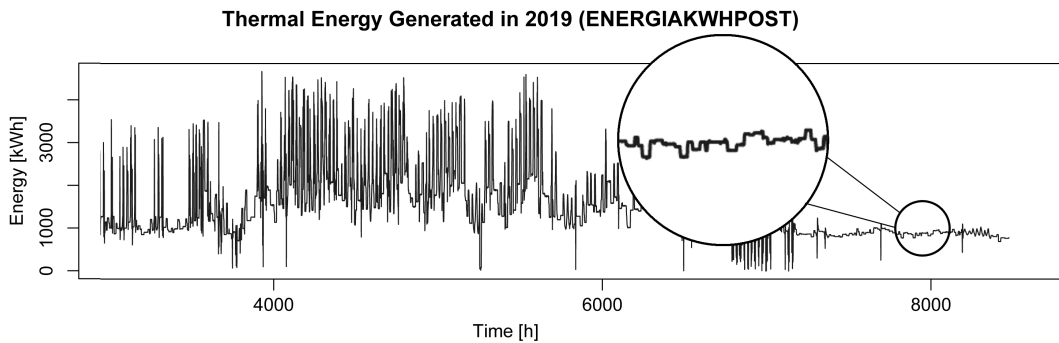


Figure 6: Detail of the thermal generation showing behavior after installation of frequency inverter in the EF4 chiller, after approx. 5000 hours, in 2019.

188 The operation of the screw type chiller is similar to a centrifugal chiller, in that operation  
189 ceases once it reaches the set-point. The main difference is that if the screw chiller has a fre-  
190 quency inverter installed in the modulation, it begins operating once this point is reached.  
191 The inverter acts directly on the power supplied to the compressor, reducing the electrical  
192 power injected and saving more energy. In addition, the minimum thermal power that the  
193 chiller can provide can be reduced before it has to be stopped. This optimization signifi-  
194 cantly reduces the number of starts and stops as shown in Figure 17, starting in the 35<sup>th</sup>  
195 month (November 2019). The thermal energy graph is flattened, as can be appreciated in  
196 Figure 6, and the generation of cooling energy is adapted to the demand, especially during  
197 the periods before and after the Summer, in which EF4 is the pre-established chiller because  
198 of its power capacity.

### 199 3.4. Proposed predictive control schema

200 The activity of the hospital's water-cooled generators was improved by implementing  
201 a predictive model of cooling demand within the BMS control system that anticipates deci-  
202 sions. The incorporated control scheme is depicted in Figure 7. The prediction model was  
203 trained with real historical data from previous years.

204 Before implementation, the BMS controlled the starting and stopping of the chillers  
205 through the set-point temperature exclusively. With the new control scheme the prediction  
206 model foresees the maximum thermal energy demanded in the cooling system for the next

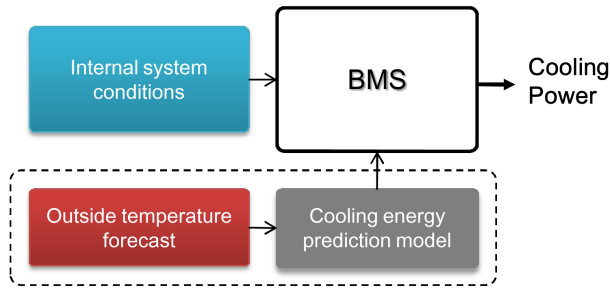


Figure 7: Control scheme. The cooling-energy prediction model communicates to the BMS the maximum thermal demand for the next day. The model reads the weather forecast conditions for the day ahead.

207 day. This allows decisions to be made ahead of time for the BMS, such as the maximum  
 208 number of chillers necessary or scheduling the cooling towers. To do this, a script devel-  
 209 oped in R language is executed daily. This program reads the internal system and external  
 210 variables, predicts the energy demand for the next 24 hours and communicates it to the  
 211 BMS.

212 The weather conditions for the coming hours (temperature, relative humidity, etc.) are  
 213 obtained from the climatological model of the Spanish National Meteorological Agency  
 214 (AEMET). The data is loaded from an XML file that is updated daily [29]. It should be  
 215 noted that these temperatures are predicted and subsequently can drag errors into the dem-  
 216 and model results, as can be observed in the difference between the predicted and real  
 217 temperatures in Figure 8.

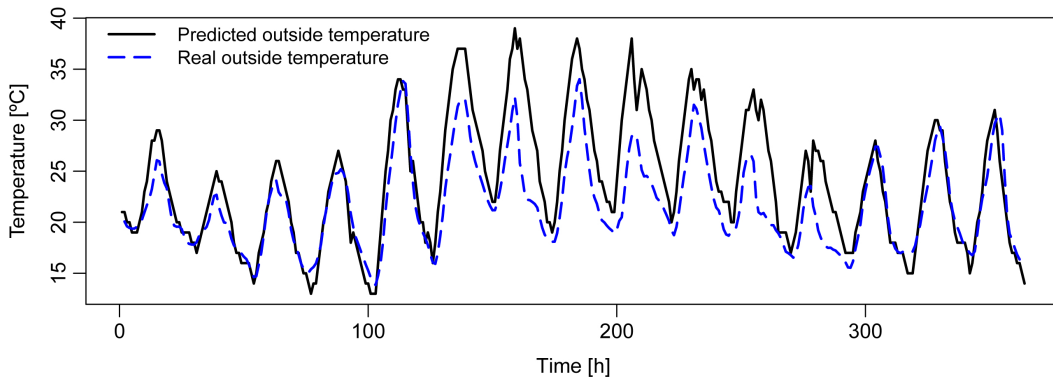


Figure 8: Outside temperature (TEXT) registered in BMS versus Forecasted temperature by AEMET model, 1st to 15th of August 2020.

218 Once the script reports the results of the forecasted cooling-energy demand for the day  
 219 ahead, the maximum demand is predicted and communicated to the BMS by an analog  
 220 signal transducer. Four possible system states have been established for the maximum  
 221 demand of the next day, as depicted in Figure 9:

- 222 - STATE 1, covered by the 1 MW chiller (EF4).
- 223 - STATE 2, covered by one of the 3.5 MW chillers (EF1, EF2 or EF3).

- 224 - STATE 3, covered by a combination of the 1 MW and one of the 3.5 MW chillers(EF4  
 225 + EF1, EF2 or EF3).
- 226 - STATE 4, covered by two of the 3.5 MW chillers.

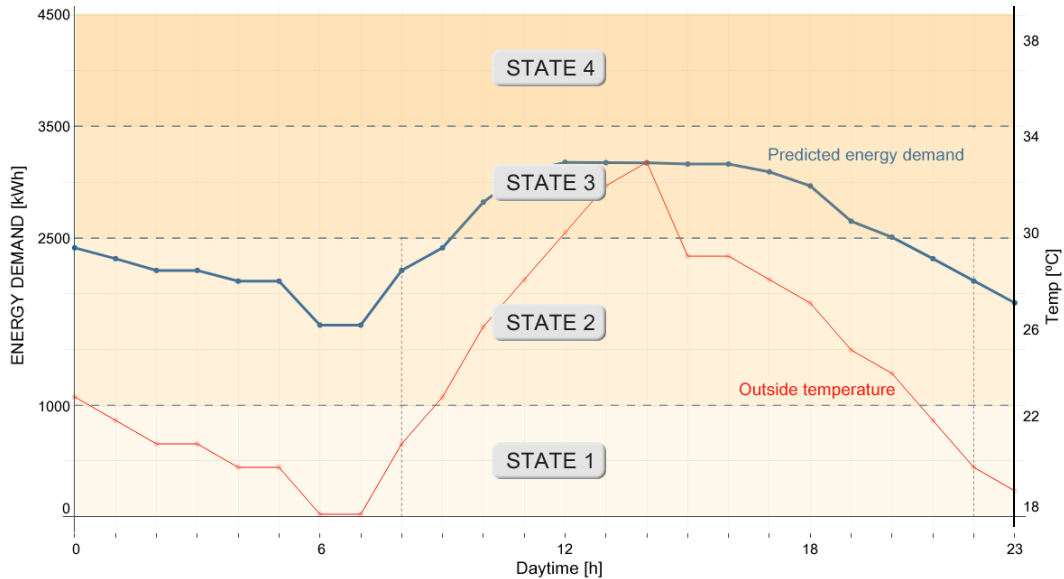


Figure 9: Energy Demand States based on the rank of the maximum energy demand for the next day.

227 In May 2020 the machine learning model that forecasts the maximum energy demand  
 228 for the cooling system was included within the BMS. A logger software was also incorpo-  
 229 rated to register data and render graphs.

### 230 3.5. Dataset

231 The Knowledge Discovery in Databases (KDD) methodology was used to develop the  
 232 forecasting model. During the process, three generations of models were created.

- 233 1. The first-generation models was tested in March 2019 [30].
- 234 2. A second generation of models was developed in December 2019 [31].
- 235 3. And finally, a third generation was created and included within the new control  
 236 scheme in May 2020.

237 The following sections describe the processes for extracting information and creating  
 238 the third-generation models, which are very similar to the previous generations.

#### 239 3.5.1. Data extraction

240 The data was extracted from the *BMS Sauter NovaPro Open* software since the beginning  
 241 of this study in 2017 (Table 1).

Table 1: Control system variables of the BMS

Short name	Description
EF1 to EF4	EF1 to EF4 - Status
TIMP	Cold-ring-drive temperature[°C]
TEXT	Exterior temperature of power installation building [°C]
TCONSIG	Calculated set-point of the regulation for cold-production drive [°C]
RH	Relative humidity [%]
TENEF1 to 4	Water temperature at the inlet of the EF1 to EF4 [°C]
TSALEF1 to 4	Water temperature at the outlet of the EF1 to EF4 [°C]

### 242 3.5.2. Data preprocessing

243 The preprocessing entailed, among others, the following actions (common in KDD pro-  
244 cesses):

- 245 1. Data Cleaning: Filling in or dropping missing values.
- 246 2. Data Integration: Averaging measurements by hour.
- 247 3. Data Transformation: The generated cooling energy (ENERGYKWHPOST) was cal-  
248 culated from the combination of other control system variables. This new feature  
249 was converted to energy [kWh] rather than instantaneous power [kW]. To smooth  
250 the noise, the final target, ENE\_GAUSSFILT11, was obtained by filtering ENERGYK-  
251 WHPOST with a Gaussian function that used a window size of 11 hours.
- 252 4. Feature and Model Selection: GAparsimony R package was used to simultaneously  
253 select the most important attributes and algorithm's parameters. The objective was  
254 to obtain parsimonious models with high accuracy and low complexity (more robust  
255 against noise and process changes, and easier to maintain).

### 256 3.5.3. Final dataset

257 In order to improve the first two generations and, according to [9, 11, 15], two new  
258 variables were included in the third generation: time and relative humidity (RH).

259 The final selection of attributes was:

Table 2: Attributes selected for testing the forecast models.

Variable	Description
ENE_GAUSSFILT11	Target feature
time	Time of measurement
month	Month of measurement
day_of_week	Day of the week
Is_holiday	Boolean variable for holiday
TIMP	Instant impulsion temperature
TEXT	Instant outside temperature
TMEAN	Average daily temperature
TMAX	Maximum daily temperature
TMIN	Minimum daily temperature
RH	Relative humidity [%]



260 The set-point temperature of the cooling water (TCONSIG) was not selected because it  
 261 was linearly related to the outside temperature (TEXT), as can be observed in Figure 3.

### 262 3.6. Parsimonious Modeling

263 The search for parsimonious models (low complexity models) is one of the current chal-  
 264 lenges in the field of Machine Learning (ML). Among models of a similar degree of pre-  
 265 cision (accuracy), choosing those that are less complex is recommended, given that they  
 266 will be better at generalizing the problem, perform more robustly against noise and dis-  
 267 turbances; and they are easier for experts to interpret, and less expensive to maintain and  
 268 update. Mechanisms used within KDD processes such as regularization or feature selection  
 269 make valuable contributions in this regard.

270 In this study, training and selecting the best parsimonious models was conducted us-  
 271 ing the GAparsimony methodology. This methodology performs a search for parsimonious  
 272 machine learning models through optimization with genetic algorithms (GA). The final  
 273 objective is to obtain models that are high in precision, yet low in complexity, using fea-  
 274 ture selection (FS), hyperparameter optimization (HO), and parsimonious model selection  
 275 (PMS). In GAparsimony, the PMS of the best individuals of each generation is carried out  
 276 in two steps: selecting the most accurate models and, from them, choosing those with the  
 277 least complexity.

278 In this study, the three ML algorithms that showed the best results in previous tests  
 279 were selected: artificial neural networks (ANN), support vector machines for regression  
 280 (SVR) with kernel based on radial basis functions (RBF), and extreme gradient boosting  
 281 machines (XGB). The final selected model was a weighted blending of the two best models  
 282 obtained with ANN and SVR. For the third generation, the use of the XGB model was  
 283 ruled out as the improvement it provided was minimal when compared to the significant  
 284 computing effort it required. All the experiments were implemented with the GAparsimony  
 285 [32] package developed in the R language.

### 286 3.7. GAparsimony settings

287 To perform GA optimization with GAparsimony, it is necessary to define the chromo-  
 288 somes of each individual to be trained with the corresponding machine learning algorithm.  
 289 In this methodology, the chromosome is defined by a combination of the algorithm’s train-  
 290 ing parameters and the input attributes selected for that individual. In particular, for the  
 291 SVR and ANN algorithms, each individual  $i$  of each generation  $g$  is defined by  $\lambda_g^i$  chromo-  
 292 some formed by the combination of two vectors  $P$  and  $Q$ :

$$\begin{aligned}
 SVR(\lambda_g^i) &= [P(cost, gamma, epsilon), Q] \\
 ANN(\lambda_g^i) &= [P(size, decay, num\_epochs), Q]
 \end{aligned}
 \tag{1}$$

293

294 where the values of the vector  $P$  correspond to the training parameters of the algorithm,  
 295 and  $Q$  corresponds to a vector of probabilities used for the selection of each input attribute  
 296  $j$  if  $q_j \geq 0.5$ .  
 297

298 As a function of  $J$  (fitness function), GAparsimony uses the Root Mean Squared Error  
 299 (RMSE) obtained with the validation database,  $RMSE_{val}$ . The RMSE error measured with  
 300 the test database,  $RMSE_{tst}$ , is used to check the generalizability of the model. Finally, the

301 complexity of the model is defined by  $N_{FS}$ , the number of attributes selected. This mea-  
302 sure of complexity has proven to be very effective in past experiences when searching for  
303 parsimonious models with GAParsimony [24, 25, 26, 27].

304 The optimization process with GAParsimony genetic algorithms was defined with a pop-  
305 ulation of 40 individuals evaluated in 100 iterations but with a stop criterion if the  $RMSE_{val}$   
306 error did not improve in 20 consecutive generations. The selection process used 20% of the  
307 best individuals (elite individuals) and was based on a two-step algorithm: In the first step,  
308 the selected models were ordered in an increasing manner based on the  $RMSE_{val}$  error. In  
309 the second step, the individuals with similar values of  $RMSE_{val}$  were re-ordered according  
310 to their lower complexity. This helped promote those less complex solutions (simpler be-  
311 cause they have fewer variables) to the top positions. In this second step, two individuals  
312 were considered similar if the absolute difference of their  $RMSE_{val}$  was less than a  $ReRank$   
313 parameter, defined by the user. In this study, and after several experiments,  $ReRank$  was  
314 set at 0.1 as it showed a satisfactory balance between complexity and  $RMSE_{val}$ .

315 After selecting the best individuals of a generation (the elite population), GAParsimony  
316 performs the traditional processes of crossing the chromosomes of the best individuals to  
317 create the next generation of individuals, as well as chromosome mutation to create more  
318 diversity of solutions in later generations. The crossover function for the  $P$  vector of the  
319 chromosomes was heuristic blending with  $/alpha = 0.1$ . For the  $Q$  vector of the chromo-  
320 somes, *random swapping* was performed. In this case, the elite individuals of the previous  
321 generation also pass on to the new generation.

322 The first generation of individuals is created randomly, but with 90% of the characteris-  
323 tics of the individuals selected. This allows the search for models to start with models that  
324 have a high number of entries.

325 Finally, the mutation is applied to the chromosomes of the new generation, except for  
326 the two best individuals. For the  $P$  vector of chromosomes, a random variation of 10% of  
327 the values is performed. In the case of vector  $Q$ , the probability of changing 0 to 1 was  
328 set at 10% in order to facilitate the reduction of the number of attributes in subsequent  
329 generations.

### 330 3.8. Energy demand model

331 To calculate the 3<sup>rd</sup> generation of models, data was collected from April 2018 to Decem-  
332 ber 2019. Prior data was removed due the relevant improvements that went into effect at  
333 that time, as shown in Figure 10. The training dataset corresponded to the period between  
334 January 2018 and February 2019. The validation database was defined to the even weeks  
335 between March 2019 and December 2019, and the test database to the odd weeks of the  
336 same period.

337 GAParsimony was used to choose the best parsimonious models trained with SVR and  
338 ANN algorithms, by adjusting the algorithm's parameters, selecting the most relevant fea-  
339 tures and choosing the best parsimonious solution. Table 3 shows the best SVR and ANN  
340 models:  $RMSE_{val}$  and  $RMSE_{tst}$ , selected features with the percentage of appearance in the  
341 elitist models during the last generations, model complexity ( $N_{FS}$ ), and the parameters of  
342 the best-tuned algorithm.

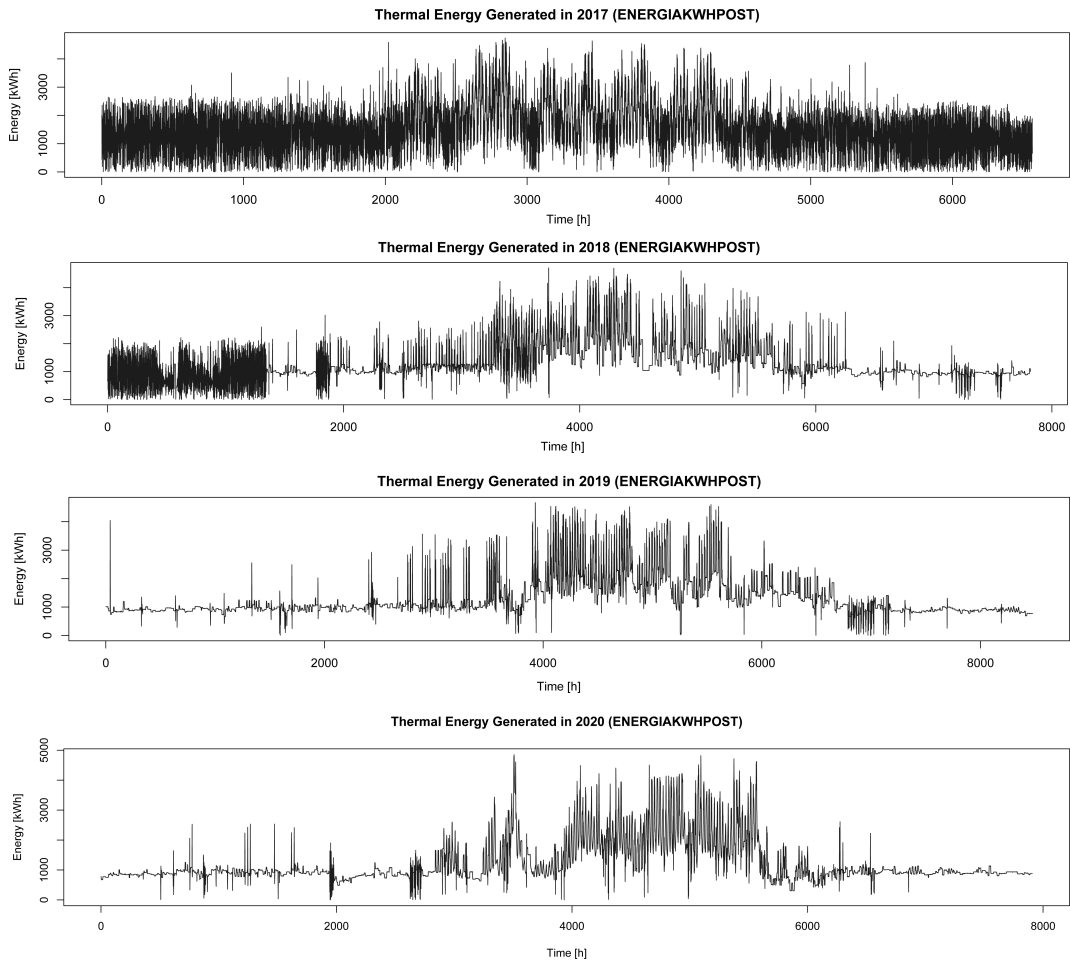


Figure 10: Evolution of energy generated in the cooling-water facility (ENERGIKWHPOST) from 2017 to 2020.

Table 3: Best models with RMSE errors, features used and their percentage of appearance in the group of elite models within the optimization process with genetic algorithms, complexity, generation and parameters.

	SVR		ANN	
$RMSE_{val}$	<b>222.95</b>		226.04	
$RMSE_{tst}$	<b>256.08</b>		264.02	
	used	% appear.	used	% appear.
<b>time</b>	<b>1</b>	99.7	<b>1</b>	100
<b>month</b>	<b>1</b>	99.6	<b>1</b>	98.6
day_of_week	0	11.8	0	11.5
Is_holiday	0	1.9	0	7.7
TIMP	0	13.7	<b>1</b>	99.2
<b>TEXT</b>	<b>1</b>	99.6	<b>1</b>	100
<b>TMEAN</b>	<b>1</b>	99.5	<b>1</b>	96.4
<b>TMAX</b>	<b>1</b>	63.4	<b>1</b>	95.8
TMIN	0	8.5	0	11.9
RH	0	32.2	0	11.1
Complexity	5		6	
Parameters	expcost	-0.014	size	33.95
	gamma	0.331	decay	200.04
	epsilon	0.048	maxit	708.13

343 SVR Model: The best SVR model was obtained with 5 features: time (*time*); month  
344 (*month*); and the outside (*TEXT*), averaged (*TMEAN*), and maximum (*TMAX*) daily temper-  
345 ature. Figure 11 shows the evolution for the most elite population of the best  $GA_{parsimony}$   
346 iteration for SVR model. White and gray box-plots represent the  $RMSE_{val}$  and  $RMSE_{tst}$   
347 evolutions respectively. Continuous and dash-dotted lines indicate the best individual er-  
348 ror for validation and test of each population. The gray area covers the range of features of  
349 most elite individuals, and the dashed line indicates the minimum number of features  $N_{FS}$   
350 (right axis).

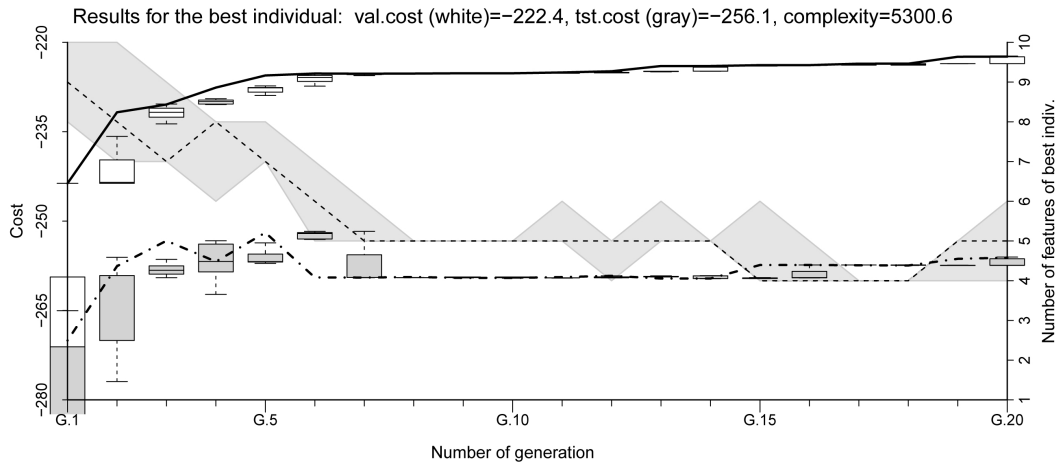


Figure 11: Evolution of the errors of the most elite solutions for SVR algorithm.

351 ANN Model: The best ANN model converged in 2 generations with 6 features: time  
 352 (*time*); month (*month*); and the temperatures of the ring (*TIMP*), outside (*TEXT*), averaged  
 353 (*TMEAN*), and maximum daily (*TMAX*). ANN errors were slightly higher than those of the  
 354 SVR model. Figure 12 displays the evolution of the ANN model.

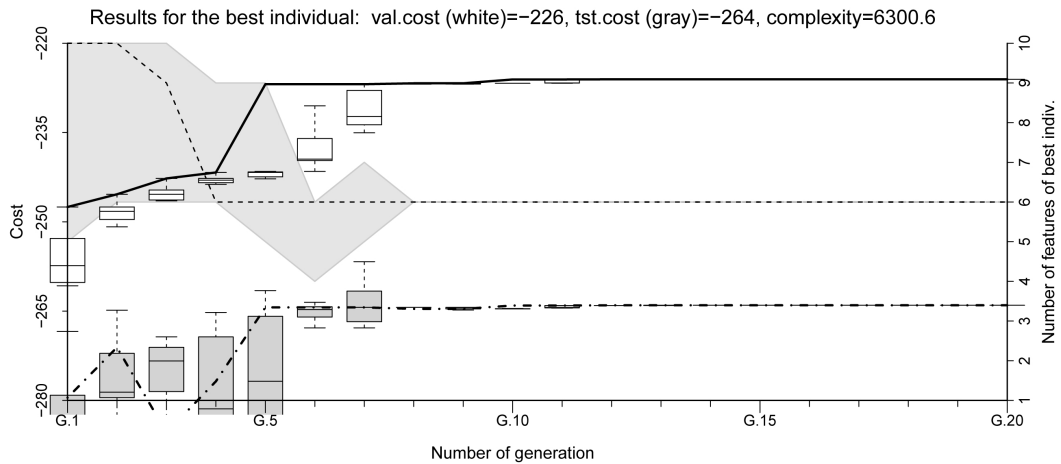


Figure 12: Evolution of the errors of the most elite solutions for ANN algorithm.

355 HYBRID Model: The best SVR and ANN models were combined to obtain a *blending*  
 356 *model* by weighting the predictions as follows,

$$\text{Hybrid\_Model} = (w1 * \text{SVR} + w2 * \text{ANN}) / 2 \quad (2)$$

357 The weights were optimized to reduce the  $RMSE_{val}$  and obtain this solution:

$$Hybrid\_Model = (1.651619 * SVR + 0.348381 * ANN) / 2 \quad (3)$$

358 Table 4 shows the improvement of  $RMSE_{val}$  and  $RMSE_{tst}$  of the hybrid model versus  
 359 single models. The error rate was slightly better in the ensemble model than the best single  
 360 model (SVR). This hybrid model reduces errors compared to the second generation hybrid  
 361 model. And in addition, it was further simplified since the previous one was composed  
 362 of 3 models (SVR, ANN, XGBoost), and it is less complex because it uses less features.  
 363 Therefore, this model is easier to maintain and more robust against noise.

Table 4: Ensemble validation and test errors versus single models.

	SVR	ANN	HYBRID
$RMSE_{val}$	221.95	226.04	<b>220.86</b>
$RMSE_{tst}$	256.08	264.02	<b>253.20</b>
complexity	5	6	5+6



Figure 13: Combined prediction for the Hybrid model.

364 As described in Section 3.2, the quality of data logged improved significantly as a result  
 365 of the installation of the LON cards. The graphs in Figures 14 compare the registered thermal  
 366 energy generated (data obtained from the LON cards) to the energy demand predicted  
 367 by the ensemble model (which uses the data predicted by AEMET as input). Furthermore,  
 368 these graphs show the influence of the outside temperature on the demand in the dotted  
 369 line: its impact increases when the outside temperature TEXT is more extreme (during July  
 370 and August). Although the data that were finally used for modeling were extracted from  
 371 the BMS sensors instead of that from LON cards, the prediction obtained is very close to

372 the registered demand.

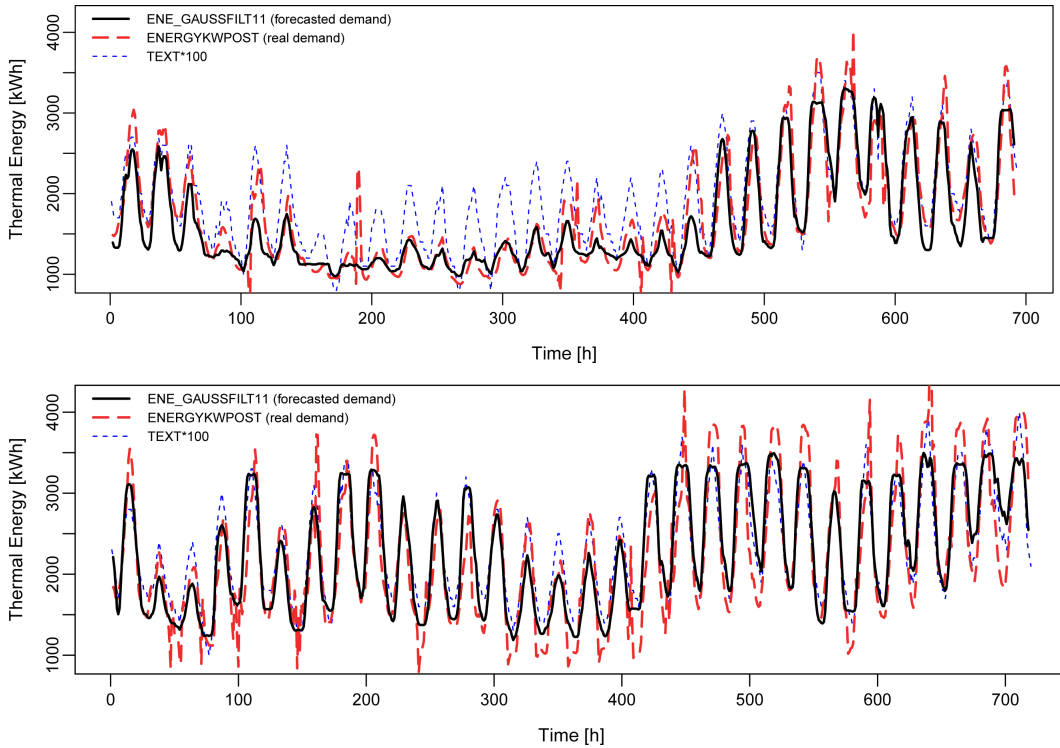


Figure 14: Forecasted energy demand (ENE\_GAUSSFILT11) versus thermal energy generated (ENERGYKWPOST) obtained from LON cards, June and July of 2020.

## 373 4. Results

### 374 4.1. Energy savings

375 The electrical energy logged made it possible to compare the annual energy savings  
376 obtained before and after the model was implemented. The data was extracted from the  
377 readings of the electrical power meter located in the hospital's power plant. This meter also  
378 measured other electrical consumption from heating and lightning. Nevertheless this data  
379 is valid for this study because the cooling generation system is the most energy-intensive  
380 installation in the building, while heating or lightning have a stable demand over time.  
381 Moreover, electrical meters were installed in every chiller, but they were not integrated  
382 until the 5<sup>th</sup> optimization of the system.

383 The method of cooling degree days (CDD) was used to normalize the consumptions for  
384 a more adequate comparison. For this calculation the temperature of 17 °C was selected  
385 as the base temperature, Figure 15 shows the variation of energy that increases once this  
386 base temperature is exceeded. Below this temperature, the cooling system stabilizes at  
387 an almost constant power of less than 1 MW (approximately 800 kW). That is the reason  
388 why in the winter season the EF4 screw chiller is able to supply enough energy to the  
389 cooling system. The meteorological data for the study was obtained from the official La



390 Rioja Government weather station [33], with data validated in accordance with the Spanish  
 391 UNE 500540 standard.

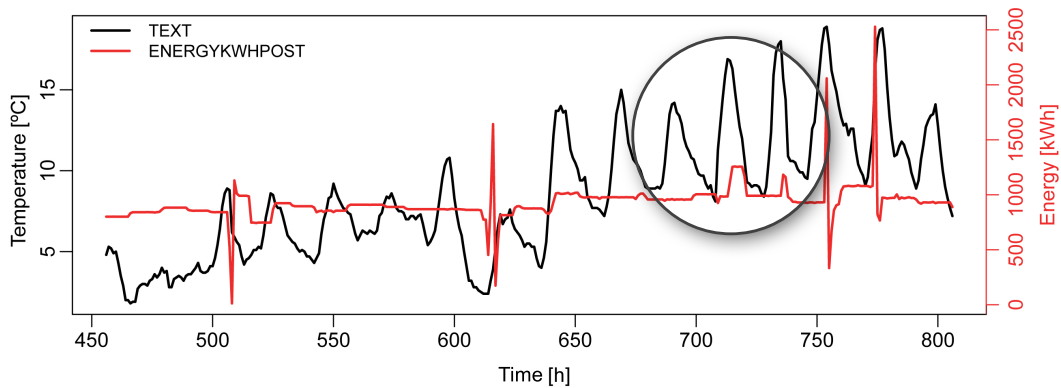


Figure 15: Outside temperature of 17 °C was chosen as the base temperature for estimating CDD since it requires additional energy to hold the cooling system. The energy peak generated can be observed inside the circle.

392 Table 5 shows the normalization of the annual electricity consumption in the building  
 393 from the year 2016 (prior to the study) to the year 2020. To perform this normalization,  
 394 the average degree days  $CDD_{17}$  in the interval 2016 – 2020 (which was 587.3 degree days),  
 395 multiplied by each annual value of  $Energy/CDD_{17}$  provides the normalized energy for  
 396 each year.

Table 5: Normalized energy per year [kWh] previous and over the course of the study, based on  $CDD_{17}$ .

Year	$CDD_{17}$	Energy [kWh]	Energy/ $CDD_{17}$	Normalized E. [kWh]
2016	590	5,968,990	10,119	5,942,682
2017	597	6,258,184	10,483	6,156,502
2018	576	6,124,609	10,629	6,242,594
2019	620	5,864,247	9,455	<b>5,553,164</b>
2020	553	6,400,075	11,569	6,794,584

397 The average cost of electrical energy during the 2017-2020 period for this building sup-  
 398 plied from a 66 kV high voltage substation is  $0.0988521 EUR/kWh$ . Depending on whether  
 399 the comparison is between the year 2016, prior to the study, or 2017, the first year of the  
 400 study, and the year 2019, the energy savings obtained by implementing this methodology  
 401 represent between 7% and 10%, which indicates economic saving of between 38,504EUR  
 402 and 59,641EUR per year, as shown in Table 6.

Table 6: Estimated savings thanks to application of the methodology.

Year	Saving (%)	Saving (EUR)
2016 vs 2019	7%	38,504.63
2017 vs 2019	10%	59,641.20

403 In order to evaluate the behavior of the plant during this year (2020, the year when  
 404 the predictive system was implemented), the monthly evolution should be analyzed in the  
 405 months of higher degree days *CDD17*, which are July and August, where the comparison  
 406 of normalized data is more descriptive, Table 7.

Table 7: Normalized Energy of most demanding months [kWh], monthly *CDD17*.

Year	CDD17	July	CDD17	August
2016	177.5	691,762	180.2	627,752
2017	176.9	715,953	160.6	738,306
2018	183.8	713,190	185.9	671,673
2019	211.2	638,511	180.2	686,522
2020	180.7	<b>675,942</b>	164.0	<b>711,752</b>

407 Higher electrical consumption (+22.3%, +122,716 EUR) was observed during the year  
 408 2020. The reason is that plant operations were atypical since all areas of the hospital  
 409 equipped with Air Handling Units (AHU), see Figure 16, were configured to avoid air  
 410 recirculation and increase ventilation flow to prevent the spread of COVID-19 [34].

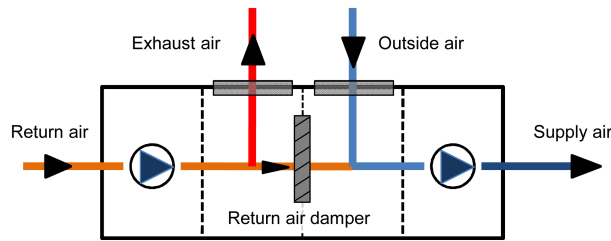


Figure 16: AHU internal scheme. The SARS-CoV-2 virus general recommendation is to avoid central recirculation by closing the recirculation dampers either using the BMS or manually.

#### 411 4.2. Measurement of the number of starts per chiller

412 The number of starts should be reduced as much as possible, especially in chillers not  
 413 equipped with inverter systems. An excessive number of starts can damage internal parts,  
 414 and every start generates an electrical peak that may affect surrounding installations.

415 The results of measurements of the number of starts per chiller are shown in Table 8  
 416 summarizing measurements by year and chiller. If the year 2017 is compared with 2019,  
 417 the total number of starts decreased by 82.7%.

Table 8: Number of starts per chiller from 2017 to 2020 (\* Chiller EF4 was damaged during 2017).

Year	EF1	EF2	EF3	EF4	TOTAL	Reduction
2017	1.911	783	1.234	0(*)	<b>3.928</b>	
2018	971	210	137	498	<b>1.816</b>	53,8%
2019	155	122	196	206	<b>679</b>	82,7%
2019	91	177	192	427	<b>887</b>	77,4%

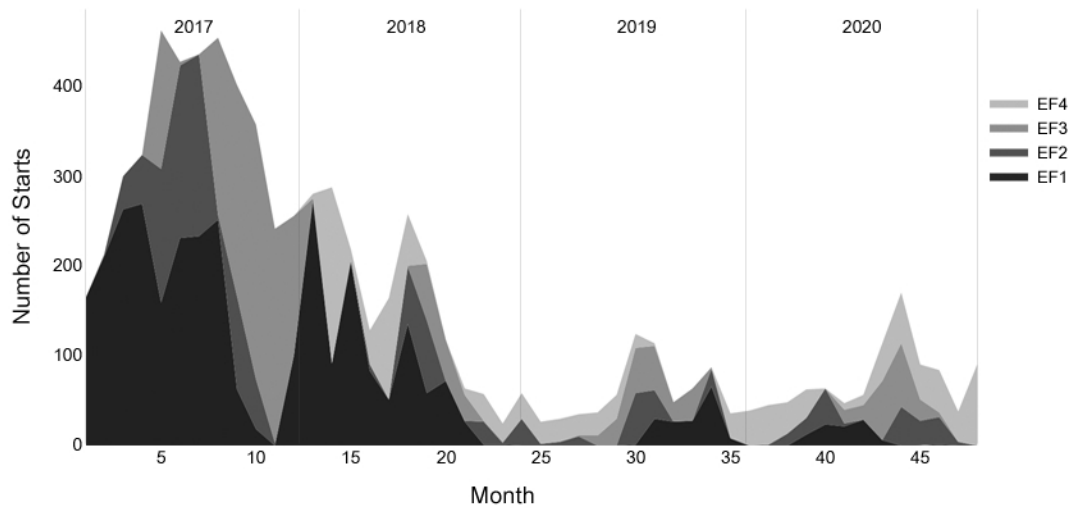


Figure 17: Number of starts per chiller from 2017 to 2020. The diagram shows the notable reduction in the number of chiller starts thanks to optimizations made to the system during the process.

418 In order to be able to compare the evolution of the number of starts during the current  
 419 year 2020, Table 9 indicates the total sum of starts of all the chillers per month. As can be  
 420 observed, in the year 2020 there have been more starts due to the night programming that  
 421 the EF4 chiller activated. This action was carried out in a controlled manner and improves  
 422 energy efficiency since this chiller gives its maximum Energy Efficiency Ratio (EER) in loads  
 423 within that range.

Table 9: Total number of chiller starts for each month and each year. The number of starts since the model was implemented is marked in bold.

Year	Jan	Feb	Mar	Apr	May	Jun	Jul	Aug	Sep	Oct	Nov	Dec
2017	159	207	292	315	450	416	424	442	391	348	235	249
2018	273	280	213	125	160	251	200	115	62	56	24	57
2019	26	29	34	36	55	121	111	47	62	85	35	38
2020	44	47	61	62	<b>46</b>	<b>55</b>	<b>111</b>	<b>166</b>	<b>88</b>	<b>82</b>	<b>37</b>	<b>88</b>

## 424 5. Conclusions

425 This methodology reworked the hospital's cooling system and solved problems that  
 426 had plagued the system in the past. Optimizing the control system by adjusting paramet-  
 427 ers (such as set-point temperature and minimum machine working time) led to the most  
 428 significant reduction in the number of chiller starts. Furthermore, implementing the BMS of  
 429 a cooling-demand prediction model allowed plant operations and performance to be opti-  
 430 mized. Thanks to this system, the maximum cooling energy demand for the next day can be  
 431 forecasted, and therefore, the BMS system can establish the number of chillers necessary. In  
 432 addition, this model provides a daily schedule for plant maintenance and a self-generated  
 433 report in R script.

434 To develop the blended prediction model, the GAparsimony methodology facilitated op-  
435 timization. In the final models, the XGBoost model was discarded because its high level of  
436 resource consumption was not compensated for by the improvements it offered. In the  
437 models that make up the final ensemble (SVR and ANN), it should be noted that the com-  
438 mon features influencing the predictions were: time, month, outdoor temperature, average  
439 temperature and maximum daily temperature. The prediction model behaves effectively,  
440 although in the months with the highest cooling energy demand (July and August), it is a  
441 conservative model and the feature "outside temperature" may have better correlation than  
442 the ensemble model (the model would not be overtrained). On the other hand, it was ob-  
443 served that the external model that implements the weather-forecast information (outdoor  
444 temperature, average temperature and maximum daily temperature) can drag errors into  
445 the prediction results.

446 Improvements in the data acquisition system enhanced the accuracy of the data from the  
447 chillers. However, since this improvement occurred at the end of the optimization process,  
448 the last models made did not include the more accurate data. These acquisition systems  
449 have improved communication with the chillers, allowing the maximum working power  
450 to be fine-tuned, which contributes to expanding cooling power, and reducing the electrical  
451 demand of the chillers by improving modulation. What's more, the addition of electrical  
452 meters in each chiller would further enrich our knowledge of plant efficiency.

453 Regarding the improvements made to the physical system, it is worth highlighting the  
454 significant improvement in the modulation of the screw chiller after an inverter system was  
455 installed, which allowed the plant to work at maximum energy efficiency and significantly  
456 reduced the number of starts and electrical demand. In the last year of the study, the total  
457 number of starts was increased deliberately due to the implementation of time schedules  
458 for higher efficiency.

459 The methodology has achieved energy savings between 7% and 10%, but the most re-  
460 markable effect was the improvement in the overall performance of the plant. The unex-  
461 pectedly greater energy demand due to increased ventilation to prevent the spread COVID-  
462 19 obviously impacted this study. Hence, the electrical consumption data from 2020 (+22.3%  
463 as compared to 2019) cannot be compared in terms of savings derived from implementing  
464 the prediction model.

465 The optimization of the plant and the KDD process are long-term procedures; the present  
466 work was conducted over the course of more than 3 years. In order to apply this method-  
467 ology in similar hospitals, it would be necessary to compile a database period of at least  
468 one year. Hence, it is exceedingly difficult to implement this methodology from scratch in  
469 a short period of time.

470 In terms of future ways to further improve the cooling plant within the same line of  
471 research, the forecasting model should be revisited using the data obtained from the LON  
472 cards installed in the chillers after a period of at least one year, and once the special mea-  
473 sures implemented due to COVID-19 are lifted. The energy efficiency of the plant should  
474 be analyzed by studying the data provided by the electrical energy meters installed in the  
475 chillers. Such research would identify the most efficient conditions for each cooler. In terms  
476 of future physical improvements, there are plans to install a system that would capture  
477 surplus energy from the condensation cooling towers, which would reinforce the overall  
478 energy efficiency of the power plant.

## 479 Acknowledgements

480 We are greatly indebted to *Banco Santander* for the APPI17/04, REGI2018/41 and REGI2018/43  
481 fellowships. This study used the Beronia cluster (Universidad de La Rioja), which is sup-  
482 ported by FEDER-MINECO grant number UNLR-094E-2C-225.

## 483 References

- 484 1. United-Nations, . The paris agreement. 2016. URL: [https://unfccc.int/  
485 process-and-meetings/the-paris-agreement/the-paris-agreement](https://unfccc.int/process-and-meetings/the-paris-agreement/the-paris-agreement).
- 486 2. European-Commission, . Eu climate action. 2018. URL: [https://ec.europa.eu/  
487 clima/policies/eu-climate-action\\_en](https://ec.europa.eu/clima/policies/eu-climate-action_en).
- 488 3. European-Commission, . Energy performance of buildings. 2014.  
489 URL: [https://ec.europa.eu/energy/en/topics/energy-efficiency/  
490 energy-performance-of-buildings/overview](https://ec.europa.eu/energy/en/topics/energy-efficiency/energy-performance-of-buildings/overview).
- 491 4. IEA, . Cooling. 2019. URL: [https://www.iea.org/reports/tracking-buildings/  
492 cooling](https://www.iea.org/reports/tracking-buildings/cooling).
- 493 5. IEA, . The future of cooling. 2019. URL: [https://www.iea.org/reports/  
494 the-future-of-cooling](https://www.iea.org/reports/the-future-of-cooling).
- 495 6. Shen, C., Zhao, K., Ge, J., Zhou, Q.. Analysis of building energy consumption in a  
496 hospital in the hot summer and cold winter area. *Energy Procedia* 2019;158:3735 – 3740.  
497 URL: <http://www.sciencedirect.com/science/article/pii/S1876610219309270>.  
498 doi:<https://doi.org/10.1016/j.egypro.2019.01.883>; innovative Solutions for En-  
499 ergy Transitions.
- 500 7. IDAE, , Fenercom, . Guía de ahorro y eficiencia energética en hospitales. *Fener-*  
501 *com* 2010;329URL: [https://www.fenercom.com/wp-content/uploads/2010/11/  
502 Guia-de-Ahorro-y-Eficiencia-Energetica-en-Hospitales-fenercom-2010.pdf](https://www.fenercom.com/wp-content/uploads/2010/11/Guia-de-Ahorro-y-Eficiencia-Energetica-en-Hospitales-fenercom-2010.pdf).  
503 doi:-.
- 504 8. Geekiyanage, D., Ramachandra, T.. A model for estimating cooling energy demand  
505 at early design stage of condominiums. *Journal of Building Engineering* 2018;17:43 – 51.  
506 URL: <http://www.sciencedirect.com/science/article/pii/S2352710217303741>.  
507 doi:<https://doi.org/10.1016/j.jobe.2018.01.011>.
- 508 9. Wang, L., Lee, E.W., Yuen, R.K.. Novel dynamic forecasting model for build-  
509 ing cooling loads combining an artificial neural network and an ensemble ap-  
510 proach. *Applied Energy* 2018;228:1740 – 1753. URL: [http://www.sciencedirect.  
511 com/science/article/pii/S0306261918311103](http://www.sciencedirect.com/science/article/pii/S0306261918311103). doi:[https://doi.org/10.1016/j.  
512 apenergy.2018.07.085](https://doi.org/10.1016/j.apenergy.2018.07.085).
- 513 10. Luo, X.. A novel clustering-enhanced adaptive artificial neural network model  
514 for predicting day-ahead building cooling demand. *Journal of Building Engineer-*  
515 *ing* 2020;32:101504. URL: [http://www.sciencedirect.com/science/article/pii/  
516 S235271022030752X](http://www.sciencedirect.com/science/article/pii/S235271022030752X). doi:<https://doi.org/10.1016/j.jobe.2020.101504>.

- 517 11. Paudel, S., Elmitri, M., Couturier, S., Nguyen, P.H., Kamphuis, R., Lacarrière,  
518 B., Corre], O.L.. A relevant data selection method for energy consumption predic-  
519 tion of low energy building based on support vector machine. *Energy and Buildings*  
520 2017;138:240 – 256. URL: [http://www.sciencedirect.com/science/article/pii/  
521 S0378778816314700](http://www.sciencedirect.com/science/article/pii/S0378778816314700). doi:<https://doi.org/10.1016/j.enbuild.2016.11.009>.
- 522 12. Li, X., Yao, R.. Modelling heating and cooling energy demand for building  
523 stock using a hybrid approach. *Energy and Buildings* 2021;235:110740. URL: [http:  
524 //www.sciencedirect.com/science/article/pii/S0378778821000244](http://www.sciencedirect.com/science/article/pii/S0378778821000244). doi:[https:  
525 //doi.org/10.1016/j.enbuild.2021.110740](https://doi.org/10.1016/j.enbuild.2021.110740).
- 526 13. Saeedi, M., Moradi, M., Hosseini, M., Emamifar, A., Ghadimi, N.. Robust  
527 optimization based optimal chiller loading under cooling demand uncertainty. *Ap-  
528 plied Thermal Engineering* 2019;148:1081 – 1091. URL: [http://www.sciencedirect.  
529 com/science/article/pii/S1359431118353547](http://www.sciencedirect.com/science/article/pii/S1359431118353547). doi:[https://doi.org/10.1016/j.  
530 applthermaleng.2018.11.122](https://doi.org/10.1016/j.applthermaleng.2018.11.122).
- 531 14. Alamin, Y.I., Álvarez, J.D., [del Mar Castilla], M., Ruano, A.. An artificial neural net-  
532 work (ann) model to predict the electric load profile for an hvac system\*\*this work has  
533 been funded by the grant from the spanish ministry of economy and competitiveness  
534 (enerpro dpi 2014-56364-c2-1-r). yaser i. alamin is a fellow of the marhaba, an erasmus  
535 mundus lot 3 project. josé domingo Álvarez is a fellow of the spanish ‘ramón y cajal’  
536 contract program, co-financed by the european social fund. antonio ruano acknowl-  
537 edges the support of fct through idmec, under laeta grant uid/ems/50022/2013. *IFAC-  
538 PapersOnLine* 2018;51(10):26 – 31. URL: [http://www.sciencedirect.com/science/  
539 article/pii/S2405896318305482](http://www.sciencedirect.com/science/article/pii/S2405896318305482). doi:[https://doi.org/10.1016/j.  
540 ifacol.2018.06.231](https://doi.org/10.1016/j.ifacol.2018.06.231); 3rd IFAC Conference on Embedded Systems, Computational Intelligence and  
541 Telematics in Control CESCIT 2018.
- 542 15. Ahmad, M.W., Mourshed, M., Rezgui, Y.. Trees vs neurons: Comparison be-  
543 tween random forest and ann for high-resolution prediction of building energy con-  
544 sumption. *Energy and Buildings* 2017;147:77 – 89. URL: [http://www.sciencedirect.  
545 com/science/article/pii/S0378778816313937](http://www.sciencedirect.com/science/article/pii/S0378778816313937). doi:[https://doi.org/10.1016/j.  
546 enbuild.2017.04.038](https://doi.org/10.1016/j.enbuild.2017.04.038).
- 547 16. Jain, R.K., Smith, K.M., Culligan, P.J., Taylor, J.E.. Forecasting energy consump-  
548 tion of multi-family residential buildings using support vector regression: Investi-  
549 gating the impact of temporal and spatial monitoring granularity on performance  
550 accuracy. *Applied Energy* 2014;123:168 – 178. URL: [http://www.sciencedirect.  
551 com/science/article/pii/S0306261914002013](http://www.sciencedirect.com/science/article/pii/S0306261914002013). doi:[https://doi.org/10.1016/j.  
552 apenergy.2014.02.057](https://doi.org/10.1016/j.apenergy.2014.02.057).
- 553 17. Bagnasco, A., Fresi, F., Saviozzi, M., Silvestro, F., Vinci, A.. Electrical con-  
554 sumption forecasting in hospital facilities: An application case. *Energy & Buildings*  
555 2015;103(Complete):261–270. doi:[10.1016/j.enbuild.2015.05.056](https://doi.org/10.1016/j.enbuild.2015.05.056).
- 556 18. Ruano, A.E., Pesteh, S., Silva, S., Duarte, H., Mestre, G., Ferreira, P.M., Khos-  
557 ravani, H.R., Horta, R.. The imbpc hvac system: A complete mbpc solution  
558 for existing hvac systems. *Energy and Buildings* 2016;120:145 – 158. URL: [http:  
559 //www.sciencedirect.com/science/article/pii/S0378778816301979](http://www.sciencedirect.com/science/article/pii/S0378778816301979). doi:[https:  
560 //doi.org/10.1016/j.enbuild.2016.03.043](https://doi.org/10.1016/j.enbuild.2016.03.043).

- 561 19. Afram, A., Janabi-Sharifi, F., Fung, A.S., Raahemifar, K.. Artificial neural network  
562 (ann) based model predictive control (mpc) and optimization of hvac systems: A state  
563 of the art review and case study of a residential hvac system. *Energy and Buildings*  
564 2017;141:96 – 113. URL: [http://www.sciencedirect.com/science/article/pii/  
565 S0378778816310799](http://www.sciencedirect.com/science/article/pii/S0378778816310799). doi:<https://doi.org/10.1016/j.enbuild.2017.02.012>.
- 566 20. Serale, G., Fiorentini, M., Capozzoli, A., Bernardini, D., Bemporad, A.. Model  
567 predictive control (mpc) for enhancing building and hvac system energy efficiency:  
568 Problem formulation, applications and opportunities. *Energies* 2018;11(3). URL:  
569 <https://www.mdpi.com/1996-1073/11/3/631>. doi:10.3390/en11030631.
- 570 21. Husain, H., Handel, N.. Automated machine learning. a paradigm shift  
571 that accelerates data scientist productivity. 2017. URL: [https://medium.com/  
572 airbnb-engineering/](https://medium.com/airbnb-engineering/).
- 573 22. Feurer, M., Klein, A., Eggenberger, K., Springenberg, J., Blum, M., Hutter, F.  
574 Efficient and robust automated machine learning. In: Cortes, C., Lawrence, N.D.,  
575 Lee, D.D., Sugiyama, M., Garnett, R., eds. *Advances in Neural Information Processing*  
576 *Systems 28*. Curran Associates, Inc.; 2015:2962–2970. URL: [http://papers.nips.cc/  
577 paper/5872-efficient-and-robust-automated-machine-learning.pdf](http://papers.nips.cc/paper/5872-efficient-and-robust-automated-machine-learning.pdf).
- 578 23. Sanz-Garcia, A., Fernandez-Ceniceros, J., Antonanzas-Torres, F., Pernia-Espinoza,  
579 A., Martinez-de Pison, F.J.. GA-PARSIMONY: A GA-SVR approach with feature  
580 selection and parameter optimization to obtain parsimonious solutions for predict-  
581 ing temperature settings in a continuous annealing furnace. *Applied Soft Computing*  
582 2015;35:13–28.
- 583 24. Sanz-García, A., Fernández-Ceniceros, J., Antoñanzas-Torres, F., Martínez-de Pisón,  
584 F.J.. Parsimonious support vector machines modelling for set points in industrial  
585 processes based on genetic algorithm optimization. In: *International Joint Conference*  
586 *SOCO13-CISIS13-ICEUTE13*; vol. 239 of *Advances in Intelligent Systems and Computing*.  
587 Springer International Publishing; 2014:1–10.
- 588 25. Urraca-Valle, R., Sanz-García, A., Fernández-Ceniceros, J., Sodupe-Ortega, E.,  
589 de Pisón Ascacibar, F.J.M.. Improving hotel room demand forecasting with a hybrid  
590 GA-SVR methodology based on skewed data transformation, feature selection and  
591 parsimony tuning. In: Onieva, E., Santos, I., Osaba, E., Quintián, H., Corchado, E.,  
592 eds. *Hybrid Artificial Intelligent Systems - 10th International Conference, HAIS 2015, Bil-*  
593 *bao, Spain, June 22-24, 2015, Proceedings*; vol. 9121 of *Lecture Notes in Computer Science*.  
594 Springer. ISBN 978-3-319-19643-5; 2015:632–643. doi:10.1007/978-3-319-19644-2\_  
595 52.
- 596 26. Fernandez-Ceniceros, J., Sanz-Garcia, A., Antonanzas-Torres, F., de Pison, F.M.. A  
597 numerical-informational approach for characterising the ductile behaviour of the T-  
598 stub component. Part 2: Parsimonious soft-computing-based metamodel. *Engineering*  
599 *Structures* 2015;82:249 – 260. doi:[http://dx.doi.org/10.1016/j.engstruct.2014.  
600 06.047](http://dx.doi.org/10.1016/j.engstruct.2014.06.047).
- 601 27. Antonanzas-Torres, F., Urraca, R., Antonanzas, J., Fernandez-Ceniceros, J., de Pison,  
602 F.M.. Generation of daily global solar irradiation with support vector machines for



- 603 regression. *Energy Conversion and Management* 2015;96:277 – 286. doi:<http://dx.doi.org/10.1016/j.enconman.2015.02.086>.
- 604
- 605 28. Danfoss, . Guías de Selección y Aplicación. Performer Compresores scroll Sencillos,  
606 20 a 110 kW 50 - 60 Hz; 2005.
- 607 29. AEMET, . 7 days ahead weather forecasting for logroño (la rioja), spain. 2020. URL:  
608 [http://www.aemet.es/xml/municipios/localidad\\_26089.xml](http://www.aemet.es/xml/municipios/localidad_26089.xml).
- 609 30. Dulce, E., Martinez-de Pison, F.J.. Parsimonious modeling for estimating hospital  
610 cooling demand to reduce maintenance costs and power consumption. In: Pérez Gar-  
611 cía, H., Sánchez González, L., Castejón Limas, M., Quintián Pardo, H., Corchado Ro-  
612 dríguez, E., eds. *Hybrid Artificial Intelligent Systems*. Cham: Springer International  
613 Publishing. ISBN 978-3-030-29859-3; 2019:181–192.
- 614 31. Dulce-Chamorro, E., Javier Martinez-de Pison, F.. Parsimonious Modelling for Esti-  
615 mating Hospital Cooling Demand to Improve Energy Efficiency. *Logic Journal of the*  
616 *IGPL* 2021;URL: [https://academic.oup.com/jigpal/advance-article-abstract/](https://academic.oup.com/jigpal/advance-article-abstract/doi/10.1093/jigpal/jzab008/6139196)  
617 [doi/10.1093/jigpal/jzab008/6139196](https://academic.oup.com/jigpal/advance-article-abstract/doi/10.1093/jigpal/jzab008/6139196). doi:10.1093/jigpal/jzab008; jzab008.
- 618 32. Martínez-De-Pisón, F.J.. GAparsimony: GA-based optimization R package for  
619 searching accurate parsimonious models.; 2017. URL: [https://github.com/jpison/](https://github.com/jpison/GAparsimony)  
620 [GAparsimony](https://github.com/jpison/GAparsimony); R package version 0.9-1.
- 621 33. de La Rioja, G.. Agroclimatic information website la rioja spain. 2020. URL: <https://www.larioja.org/agricultura/es/informacion-agroclimatica/>.
- 622
- 623 34. Morawska, L., Tang, J.W., Bahnfleth, W., Bluyssen, P.M., Boerstra, A., Buonanno,  
624 G., Cao, J., Dancer, S., Floto, A., Franchimon, F., Haworth, C., Hogeling, J., Isaxon,  
625 C., Jimenez, J.L., Kurnitski, J., Li, Y., Loomans, M., Marks, G., Marr, L.C., Maz-  
626 zarella, L., Melikov, A.K., Miller, S., Milton, D.K., Nazaroff, W., Nielsen, P.V.,  
627 Noakes, C., Peccia, J., Querol, X., Sekhar, C., Seppänen, O., ichi Tanabe, S., Tellier,  
628 R., Tham, K.W., Wargocki, P., Wierzbicka, A., Yao, M.. How can airborne transmis-  
629 sion of covid-19 indoors be minimised? *Environment International* 2020;142:105832.  
630 URL: <http://www.sciencedirect.com/science/article/pii/S0160412020317876>.  
631 doi:<https://doi.org/10.1016/j.envint.2020.105832>.